Polymer Cross-Linking in Post-Gel Region for Continuous and Batch Reactors

C. Cozewith
Exxon Chemical Co., Baytown Polymers Center, Baytown, TX 77520

F. Teymour
Dept. of Chemical and Environmental Engineering, Illinois Institute of Technology, Chicago, IL 60616

Tetrafunctional chain coupling of polymers is an important process for introducing long-chain branching to modify flow behavior and for forming cross-linked networks. Reactor modeling for polymers branched beyond the gel point is a difficult problem because of the divergence of the moments of the MWD to infinity. A newly developed technique, numerical fractionation, based on the method of moments is applied to modeling chain coupling (cross-linking) kinetics in continuous flow stirred tank (CFST) and batch reactors. The resulting model is applicable from 0 to 100% gelation and predicts the amount of sol fraction and its molecular weight and MWD as a function of operating conditions. This technique is easier to apply to reactor simulation than others for calculating properties of polymers in the post-gel region. An examination of CFSR dynamics during reactor startup indicates a wide range of behavior depending on the critical residence time for gel formation. At residence times close to the critical, long times are needed to reach steady state, but at residence times much greater than the critical, the reactor can reach steady state in less than three turnovers. For both the batch and CFST reactors, polymer properties are determined by only two parameters: initial polymer MWD and reduced reaction time or reduced residence time. Consequently, at a given sol fraction, the molecular weight and MWD of the sol polymer are fixed. Narrowing the initial polymer MWD increases the amount of gel present at a given reaction time. Considerable differences are shown in the rate of the chain coupling reaction and properties of the sol phase between the two reactor types.

Introduction

Tetrafunctional branching chemistry is of considerable importance in the production of synthetic polymers. Low levels of branching are often deliberately introduced into polymers to modify the rheological behavior. However, if branching rate is not carefully controlled, the polymers could become branched beyond the gel point which can lead to formation of a gel phase in the reactor and a loss of polymer physical properties in end-use applications. Tetrafunctional branching kinetics are also of interest for the analysis of cross-linking and network formation. Various chain coupling initiators, for example, cationic species, cross-linking agents, or radiation, can be used to form branched polymers. This article considers chain coupling for an idealized system in which any two mers in a chain can react to form a branch.

Flory's (1947) classic study of branching reactions was based on statistical reasoning. This approach is very useful for stepwise polymerization reactions, but lacks flexibility for additional polymerization and is difficult to apply to polymerization in CFST reactors. In this latter situation, population balance methods (method of moments) are more easily applied to obtaining relationships for calculating polymer molecular weight. In an earlier article, Cozewith, Graessley, and Ver Strate (1979) used the method of moments to derive equations describing the effect of tetrafunctional coupling on polymer MW and MWD in batch and CFST reactors. These equations were applicable up to the gel point at which time the second moment of the distribution diverged to infinity. Recently, a number of articles (Mikos et al., 1986; Tobita and

Hamielec, 1988, 1989, 1992; Zhu and Hamielec, 1993; Xie and Hamielec, 1993; Okay, 1994; Teymour and Campbell, 1994; Tobita et al., 1994) have appeared proposing techniques based on the method of moments for calculating polymer properties past the gel point. The methodology developed by Teymour and Campbell (1994), which they term numerical frationation, appears to be particularly versatile and straightforward to use for determining the amount of sol fraction and the sol fraction properties.

In this article the numerical fractionation technique is applied to batch and CFST reactors to calculate the effect of chain coupling on polymer properties in both the pregel and postgel regions. For the batch reactor and the CFST reactor in the pregel period, the results are compared to those of other techniques to confirm the validity of the numerical fractionation approach. For the CFST reactor in the postgel period, new results are presented describing the properties of the cross-linked polymer and the behavior of the reactor.

Theory

We consider the intermolecular coupling of long chain polymer molecules according to the reaction

$$P_i + P_j \rightarrow P_{i+j}$$

We assume that all mers have an equal probability of reacting and ignore loop formation and excluded volume effects. The above reaction then proceeds at a rate given by

$$R_{ij} = kijP_iP_j$$

where P_i and P_j are concentrations of i and j-mers in the reactor (moles/volume) and k is the branching rate constant. Since gelation of high molecular weight polymers results from coupling of only a very small fraction of mers, we will ignore the loss of mers by reaction and assume constant total mer concentration.

The moments of the distribution are defined by

$$Q_n = \sum_{i=1}^{\infty} i^n P_i \tag{1}$$

and the number and weight average degrees of polymerization are given by

$$D_n = Q_1/Q_0$$
$$D_w = Q_2/Q_1$$

Only cross-linking, and not polymerization, reactions are considered in this study. In the initial condition, we assume the reactor, either batch or CFST, is filled with a polymer solution having a molecular weight distribution specified by $(D_w/D_n)^0$ at a given initial concentration of Q_1^0 mers/volume.

In addition, the CFST reactor is continuously fed with the same polymer solution as initially fills the reactor. The equations for the moments of the MWD in this situation were derived in the previous study (Cozewith et al., 1979). In dimensionless form the first three moments for the batch reactor are

$$-dZ_0/dt_r = Z_1^2/2(D_w/D_n)^0 \tag{2}$$

$$-dZ_1/dt_r = 0 \tag{3}$$

$$-dZ_2/dt_r = -Z_2^2 \tag{4}$$

where
$Z_n = Q_n/Q_n^0$
t = time
$t_r = t/t_c$

The critical reaction time to reach the gel point t_c is given by

$$t_c = 1/(k\,Q_1^0 D_w^0)$$

Where the superscript 0 denotes an initial condition. Note that dZ_1/dt_r is zero since chain coupling does not change the concentration of mers in the reactor. Thus

$$Z_1 = 1$$

at all times for both the batch and CFST reactors. As can be seen from these equations, the dimensionless moments Z_n are only a function of the dimensionless time t_r and the initial polymer MWD.

The equivalent moment equations for the CFST reactor are

$$-dZ_0/dt_r = Z_1^2/2(D_w/D_n)^0 - \theta_c(1-Z_0)/\theta \tag{5}$$

$$-dZ_1/dt_r = 0 \tag{6}$$

$$-dZ_2/dt_r = -Z_2^2/4 - (1-Z_2)\theta_c/\theta \tag{7}$$

where θ is the mean residence time (= reactor volume/flow rate); θ_c is the critical residence time; $t_r = t/\theta_c$.

The critical residence time for the CFST reactor, the residence time at which gel begins to form, was shown by Cozewith et al. (1979) to be

$$\theta_c = 1/\left(4kQ_1^0D_w^0\right)$$

At steady state, the derivative terms vanish from the CFST reactor equations and the dimensionless moments are a function only of θ/θ_c and $(D_w/D_n)^0$. However, in unsteady-state operation, such as during reactor startups or reactor transients, reactor behavior is also a function of t/θ_c.

The solution of Eqs. 2–4 and Eqs. 5–7 is only possible when there is no gel present. In the pre-gel regime ($t < t_c$ or $\theta < \theta_c$), the equations are readily integrated, and the key results, as presented in the previous article (Cozewith et al., 1979), are:

(1) A comparison of t_c and θ_c indicates that critical gel time in the CFST reactor is 1/4 of t_c for the batch reactor.

(2) The second moment equations (Eqs. 4 and 8) for both types of reactor diverge to infinity when the critical time ratios t/t_c or θ/θ_c are greater than 1.0.

(3) In a CFST reactor, the maximum steady-state value for D_w/D_n (at $\theta = \theta_c$) is equal to only $2(D_w/D_n)^0 - 1/4$.

(4) The time to reach steady state in CFST increases substantially as θ/θ_c approaches 1.0.

Teymour and Campbell (1994) propose extending the moment equations beyond the gel point by dividing the population of chains into various branched polymer generations.

According to their methodology, linear and unbranched polymers are considered to be zeroth generation. When two linear chains couple, a first generation branched polymer is formed. Addition of generation one polymer to generation two polymer results in a generation two polymer with an additional branch. However, when two generation one polymers couple, a generation two polymer is formed. Thus, the general rule is that a polymer of the next higher generation is formed when two chains of the same generation cross-link. Coupling of higher and lower generation chains leaves the rank of the higher generation chain unchanged, but results in broadening of the distribution for this generation.

For generations after the zeroth, the concentration of each generation initially increases as it is formed, and then decreases as it reacts to form higher generations. The concentration of the zeroth generation, of course, just decreases with time. The technique for calculating the MW of the entire polymer is to solve the material balance equations generation by generation up to a number of generations (5–10) sufficient to include almost all of the soluble fraction. Higher generations, which will have very high molecular weights and also represent a minute fraction of the sol, are included as part of the gel phase. All of the finite moments are added together to get the moments for the soluble fraction as a whole. The amount of gel is calculated by subtracting the first moment for the soluble polymer from the total first moment for the polymer. Teymour and Campbell demonstrate this method for polymerization with chain transfer to polymer.

To apply the numerical fractionation technique to tetrafunctional chain coupling, we define the species concentration as

$$P_{y,i}$$

where y is the generation number; i is the number of mers.

Then the coupling reactions are

$$P_{y,i} + P_{x,j} = P_{y,i+j} \quad y > x$$
$$P_{y,i} + P_{y,j} = P_{y+1,i+j}$$
$$P_{y,i} + P_{z,j} = P_{z,i+j} \quad y < z$$

Material balance equations for species $P_{y,i}$ in a batch reactor will contain three terms: (1) loss of $P_{y,i}$ by reaction with any other chain; (2) formation of $P_{y,i}$ by reaction of $P_{y-1,j}$ with $P_{y-1,i-j}$; and (3) formation of $P_{y,i}$ by reaction of $P_{y,i-j}$ with lower generation chains $P_{x,j}$ for $1 \le x < y$. The batch reactor material balance for generations 2 and greater is therefore

$$-dP_{y,i}/dt = k(iP_{y,i}) \sum_{x=1}^{\infty} \sum_{j=1}^{\infty} jP_{x,j} - (k/2) \sum_{j=1}^{i-1} j(i-j)P_{y-1,j}P_{y-1,i-j} - k \sum_{j=1}^{i-1} (i-j)P_{y,i-j} j \sum_{x=1}^{y-1} P_{x,j} \quad (8)$$

The factor of 1/2 in the second term is to avoid double counting in the summation. For the first generation, initial polymer we have

$$-dP_{1,i}/dt = kiP_{1,i} \sum_{y=1}^{\infty} \sum_{j=1}^{\infty} jP_{y,j} \quad (9)$$

The moments for the yth generation are defined as

$$Q_{y,n} = \sum_{i=1}^{\infty} i^n P_{y,i} \quad (10)$$

and the overall moment for both the sol and gel is

$$Q_n = \sum_{y=1}^{\infty} \sum_{i=1}^{\infty} i^n P_{y,i} \quad (11)$$

To simplify the nomenclature we also introduce

$$S_{y,j} = \sum_{x=1}^{y-1} P_{x,j} \quad (12)$$

$$R_{y,n} = \sum_{j=1}^{\infty} j^n S_{x,j} = \sum_{x=1}^{y-1} Q_{x,n} \quad (13)$$

The moment equations are obtained by multiplying Eqs. 8 and 9 by i^n and carrying out a summation for $i = 1$ to ∞. This produces the result

for $y > 1$

$$-dQ_{y,n}/dt = kQ_1Q_{y,n+1} - (k/2) \sum_{i=1}^{\infty} i^n \sum_{j=1}^{i-1} j(i-j) \times P_{y-1,j}P_{y-1,i-j} - k \sum_{i=1}^{\infty} i^n \sum_{j=1}^{i-1} j(i-j)P_{y,i-j}S_{x,j} \quad (14)$$

for $y = 1$

$$-dQ_{1,n}/dt = kQ_1Q_{1,n+1} \quad (15)$$

The double sums in Eq. 14 can be simplified to the expressions shown in Table 1. Inserting these terms into Eq. 14 yields the moment equations for the individual generations

$$-dQ_{1,0}/dt = kQ_{1,1}Q_1 \quad (16)$$

Table 1. Value of the Summation

$$\sum_{i=1}^{\infty} i^n \sum_{j=1}^{i-1} j(i-j)P_{y,i-j}P_{x,j}$$

n	Summation
0	$Q_{y,1}Q_{x,1}$
1	$Q_{y,1}Q_{x,2} + Q_{y,2}Q_{x,1}$
2	$Q_{y,3}Q_{x,1} + 2Q_{y,2}Q_{x,2} + Q_{y,1}Q_{x,3}$

$$-dQ_{y,0}/dt = kQ_1Q_{y,1} - (k/2)(Q_{y-1,1})^2 - k(Q_{y,1}R_{x,1}) \quad (17)$$

$$-dQ_{1,1}/dt = kQ_{1,2}Q_1 \quad (18)$$

$$-dQ_{y,1}/dt = kQ_1Q_{y,2} - k(Q_{y-1,1}Q_{y-1,2}) - k(Q_{y,1}R_{x,2} + R_{x,1}Q_{y,2}) \quad (19)$$

$$-dQ_{1,2}/dt = kQ_{1,3}Q_1 \quad (20)$$

$$-dQ_{y,2}/dt = kQ_1Q_{y,3} - k\left(Q_{y-1,1}Q_{y-1,3} + Q_{y-1,2}^2\right) - k(Q_{y,3}R_{x,1} + 2Q_{y,2}R_{x,2} + Q_{y,1}R_{x,3}) \quad (21)$$

Equations 17, 19 and 21 apply for y values greater than 1.

Summing Eqs. 17, 19, and 21 over the generations from 2 to ∞ and then adding the appropriate first generation moments Eqs. 16, 18 or 20 gives the total moments

$$dQ_0/dt = kQ_1^2 - (k/2)\sum_{y=1}^{\infty}(Q_{y,1})^2 - k\sum_{y=2}^{\infty}Q_{y,1}\sum_{x=1}^{y-1}Q_{x,1} \quad (22)$$

$$dQ_1/dt = kQ_1Q_2 - k\sum_{y=1}^{\infty}Q_{y,1}Q_{y,2} - k\sum_{y=2}^{\infty}\left(Q_{y,1}\sum_{x=1}^{y-1}Q_{x,2} + Q_{y,2}\sum_{x=1}^{y-1}Q_{x,1}\right) \quad (23)$$

$$dQ_2/dt = kQ_1Q_3 - k\sum_{y=2}^{\infty}\left(Q_{y-1,1}Q_{y-1,3} + Q_{y-1,2}^2\right) - k\sum_{y=2}^{\infty}\left(Q_{y,3}\sum_{x=1}^{y-1}Q_{x,1} + 2Q_{y,2}\sum_{x=1}^{y-1}Q_{x,2} + Q_{y,1}\sum_{x=1}^{y-1}Q_{x,3}\right) \quad (24)$$

Expanding the series expressions in Eqs. 22 to 24 and collecting similar moment terms produces equations that are identical to the overall moments given by Eqs. 2, 3, and 4. Thus, the numerical fractionation method alters the classification system for accounting for chains but the resulting material balance equations are exact and all polymer molecules are included.

Note in the second moment equations, Eqs. 20 and 21, a third moment term appears. As suggested by Teymour and Campbell (1994), the Saidel and Katz (1968) moment closure approximation

$$Q_3 = 2Q_2^2/Q_1 - Q_2Q_1/Q_0 \quad (25)$$

was used to relate the second and third moments for a given generation. This relationship is equivalent to

$$D_z/D_w = 2 - D_n/D_w \quad (26)$$

where D_z is the z average degree of polymerization, and it gives the correct D_z/D_w values in the limiting cases of a monodisperse MWD ($D_w/D_n = 1$) and a most probable MWD ($D_w/D_n = 2$). In this article we are primarily interested in the characteristics of the total sol fraction. When the sum for the total second moment is formed, the third moment terms cancel out (see Eq. 4) so the nature of the closure approximation for a generation should have little effect on the overall second moment of the sol. For a given generation, it is difficult to estimate errors in the moments arising from the use of the moment closure approximation, as pointed out by Saidel and Katz (1968). However, Gossage (1997) and Gossage and Teymour (1998) show that for a gelation mechanism similar to the one examined in this article, full MWDs constructed by combining the MWDs for individual generations can give good agreement with measured MWDs for branched polymers. Furthermore, for the special case of cross-linking polymers that are initially monodisperse, the numerical fractionation solution for the moments of the individual generation was shown to be in excellent agreement with an exact solution. Thus, it appears that the Saidel and Katz approximation leads to satisfactory accuracy. This closure method is expected to be adequate for relatively narrow and nonskewed distributions, and thus should be suitable for application to individual generations as defined by numerical fractionation. A derivation included in the appendix independently confirms the validity of this approximation for the linear polymer generation.

Nine generations were selected to represent the total polymer MWD. Applying Eqs. 16 to 21 to each generation results in 27 ODEs in 27 unknowns (three moment equations for each of the nine generations). The batch reactor equations are as shown in Eqs. 16 to 21 and were solved with the initial conditions

$$Q_{1,0} = Q_0^0$$

$$Q_{1,1} = Q_1^0$$

$$Q_{1,2} = Q_2^0$$

$$Q_{y,n} = 0 \text{ for } y > 1$$

which hold when the polymer present at the start of reaction is unbranched.

An initial value for D_z/D_w^0 is calculated from Eq. 25.

For the CFST reactor, we are interested in modeling reactor dynamic behavior, especially startups, as well as steady-state operation. The unsteady-state material balances are identical to the ODEs in Eqs. 16 to 21 but with the flow term

$$\left(Q_{y,n}^0 - Q_{y,n}\right)/\theta$$

subtracted from the righthand side of each equation. Since this study is limited to gelation reactions in which only unbranched polymer is fed to the reactor, the flow term reduces to $Q_{y,n}/\theta$ for all generations except the first. CFST reactor startup is assumed to proceed by: (1) filling the reactor with a solution of polymer at concentration $Q_{1,1}^0$; (2) feeding a polymer solution at the same concentration at a rate such that the residence time in the reactor is θ; and (3) at time equal zero beginning the branching reaction (such as beginning catalyst feed). The CFST reactor ODEs are then integrated from time zero to a time long enough for the reactor to reach steady state.

Steady-state results can also be obtained by setting the derivative terms to zero in Eqs. 16 to 21 and solving the corresponding set of algebraic equations. In this case, the moment equations can be solved sequentially, one generation at a time, starting with the first, and simultaneous solution of all 27 expressions is not required.

Equation Solution

The system of ordinary differential equations (ODE) for the moments in batch and continuous flow stirred reactors was integrated by means of the numerical ODE solving algorithm DDASAC (Caracotsios and Stewart, 1985) which was developed for the solution and sensitivity analysis of the differential-algebraic systems of equations. The batch reactor equations were integrated without difficulty, but the CFST equations presented problems due to the vast differences in the order of magnitude for the state variables and the fact that many of these variables are close to zero for most of the simulation which makes it difficult to stay around a steady state without considerable error accumulation. The following strategies were used to obtain successful results for the CFST reactor:

(1) After each integration step, the current solution is checked by DDASAC for convergence, appropriate step size and nonsingularity of the Jacobian. If the solution did not meet the success criteria, the integrator was restarted which forced DDASAC to recalculate the initial step size and to re-initialize the calculation of the backward integration steps. In many cases this was sufficient to let the integration proceed around problem areas.

(2) The moment values for each generation were monitored at each time step to make sure they remained positive. If negative values arose, the integrator was restarted with the negative moments set equal to zero in the initial condition.

(3) When integrating out to long times, errors tend to accumulate in the moments of generations which are close to zero in concentration for most of the time period. This was avoided by setting the relative solution tolerance (RTOL) specified to DDASAC at 1.0E-12 for the lower generations at 1.0E-08 for the higher generations. Since the concentrations of the higher generations rapidly fall to zero, the smaller value of RTOL does not affect the overall accuracy of the solution.

(4) The absolute tolerance for the solution was set at close to the machine precision (1.0E-14 vs. 1.0E-16).

Results

Calculations with the numerical fractionation model were compared to existing analytical solutions where possible to examine the accuracy of the method. In the pre-gel region, the model gave results identical to those obtained with the exact equations for both batch and CFST reactors published earlier (Cozewith et al., 1979). For a CFST reactor startup, the model also calculated a time to reach the gel point in agreement with Eq. 12 in the previous work. Past the gel point, there are no prior derivations available based on moment equations. However, Flory (1947) used statistical reasoning to obtain equations for percent gel and sol fraction properties for batch cross-linking.

He showed that the weight fraction of sol was given by

$$W_s = (1-\rho)\xi_s + \rho\xi_s^2$$

where ρ is the fraction of units in crosslinks; ξ_s is the probability that a noncross-linked unit is part of the sol fraction.

For a polymer initially having a most probable MWD, D_n and D_w for the sol depend on the parameters, I_1, I_2, and I_3 which are defined by

$$I_1 = (W_s/\xi_s)(1-p)^2/(1-pW_s/\xi_s) \tag{28}$$

$$I_2 = W_s = I_1/(1-pW_s/\xi_s) \tag{29}$$

$$I_3 = I_2(1+pW_s/\xi_s)/(1-pW_s/\xi_s) \tag{30}$$

where $p = 1 - 1/D_n^0$.

D_n and D_w for the sol are obtained from the I values with the relationships

$$D_n = W_s/(I_1 - \rho\xi_s/2) \tag{31}$$

$$D_w = (I_3/W_s)(1+\rho')/(1-\rho'(I_3/W_s - 1)) \tag{32}$$

where $\rho' = \rho\xi_s^2/W_s$.

To calculate W_s, D_n, and D_w, Eqs. 27 to 32 must be solved as a function of ρ, which depends on cross-linking rate, and p which is a function of D_n^0.

The coupling rate of mers M (mol/L) in a batch reaction is equal to

$$-dM/dt = kM^2 \tag{33}$$

and integration gives

$$M/Q_1^0 = 1/(1+ktQ_1^0) \tag{34}$$

The fraction of mers in cross-links is equal to

$$\rho = (Q_1^0 - M)/Q_1^0 = Q_1^0 kt/(1+Q_1^0 kt) \tag{35}$$

which relates ρ to the parameters that appear in the generation moment equations presented earlier.

Equation 29 can be rearranged to

$$(1-p)^2/\xi_s = \{1 - p[(1-\rho) + \beta\xi_s]\}^2 \tag{36}$$

The one real root of ξ_s that lies between 0 and 1 is given by

$$\xi_s = \left[A + 2(1-p) - A^{1/2}\sqrt{A + 4(1-p)}\right]/2A \tag{37}$$

where $A = \rho p$.

The statistical model equations were solved by selecting values for Q_1^0, t, k, and D_n^0; calculating ρ and p; and then obtaining ξ_s from Eq. 37. With these parameters established, W_s, D_n and D_w can be obtained by sequential solution of Eqs. 27 to 32. It was shown earlier from the moment equations that W_s, D_n/D_n^0 and D_w/D_w^0 are all functions of the single parameter t/t_c. This simple and useful result is not obvious from the relationships based on statistical reasoning.

D_n/D_n^0, D_w/D_w^0, and W_s calculated by the numerical fractionation method for batch cross-linking are shown in Figures 1 to 3. In the pre-gel region the results are virtually indistin-

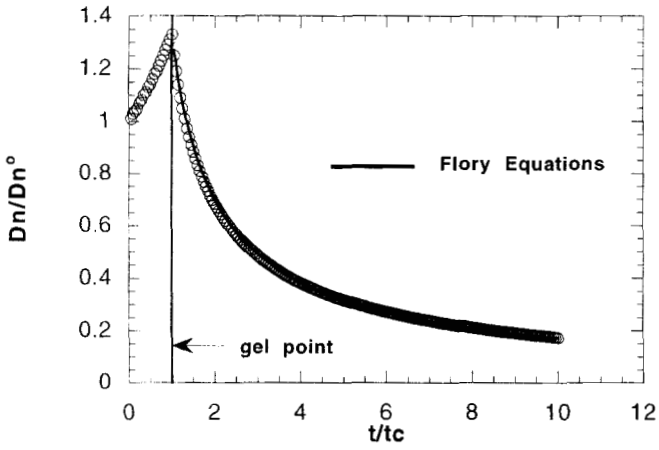

Figure 1. D_n behavior in batch cross-linking.

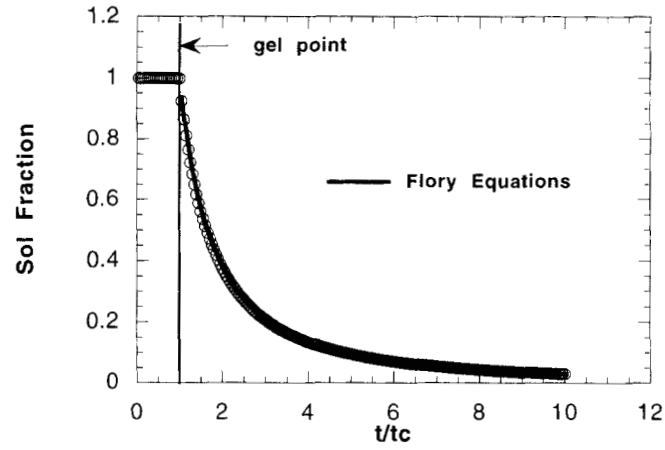

Figure 3. Sol fraction amount for batch cross-linking.

guishable from the Flory model predictions; however, in the post-gel region, differences of several percent arise (as shown in Figure 4). Not surprisingly, the discrepancy between the two predictions is only significant in the immediate vicinity of the gel point, where both methods are trying to approximate a divergent second moment and, hence, an "infinite" weight-average chain length.

The Flory approach becomes more difficult to apply when the initial MWD of the polymer cannot be simply expressed as a function of p (Charlesby, 1954). This is not the case with the numerical fractionation model, which only requires the initial value for D_w/D_n. With D_n^0 held constant, we have examined the effect of $(D_w/D_n)^0$ between 1.5 and 5.0 on the cross-linking process, and, as shown in Figure 5, at the same value of reduced time t/t_c, the percent of sol fraction decreases as initial MWD narrows. Thus, gel forms more rapidly in the post gel period with narrower MWD as a consequence of the increase in reaction rate with increasing chain length. This is a well-known effect in elastomer vulcanization. If this calculation were made with D_n^0 held constant, a different picture would emerge since t_c varies with D_w^0 (Gossage and Teymour, 1997).

The analytical solution of the moment equations in the pregel period ($t/t_c < 1$) indicates D_n/D_n^0 is a function of t_r and $(D_w/D_n)^0$, but D_w/D_w^0 depends only on t_r and is independent of the initial MWD breadth. In the post-gel region, D_w/D_w^0 for the sol fraction is not strongly affected by $(D_w/D_n)^0$ up to t_r of about 2 which corresponds to a sol fraction of 35–45% (see Figure 6). However, at higher t_r, narrowing the initial MWD raises D_w for the sol phase at the same t_r value.

As would be expected, at equal sol fraction, D_w/D_n for the sol increases with (D_w/D_n^0) (see Figure 7). Extrapolation of the curves in Figure 7 indicates the last increment of sol remaining when the gelation is complete has the same D_w/D_n as the initial, uncross-linked polymer. This, of course, is a direct result of the fact that the last remaining increment of sol must belong to the generation representing the original polymer. The fact, however, that this generation's polydispersity remains constant as it is consumed is not intuitive. At

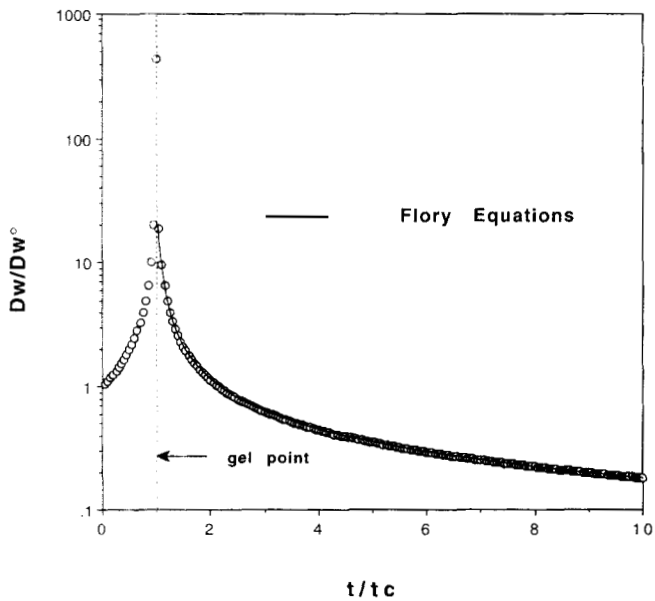

Figure 2. D_w behavior in batch cross-linking.

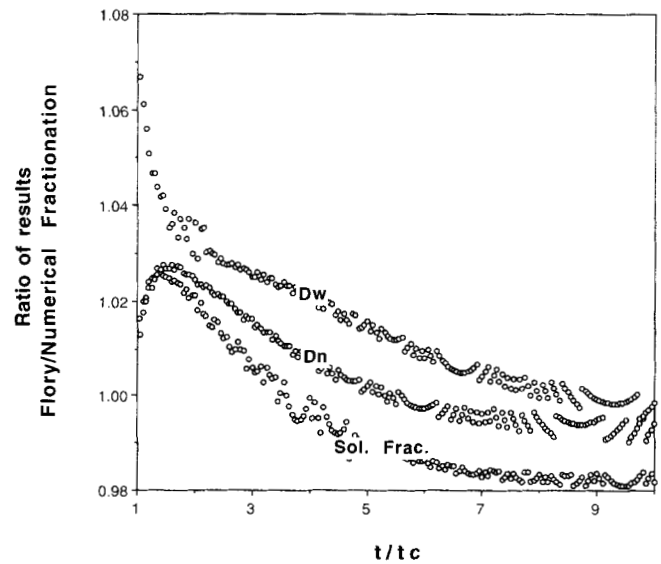

Figure 4. Batch cross-linking model comparison.

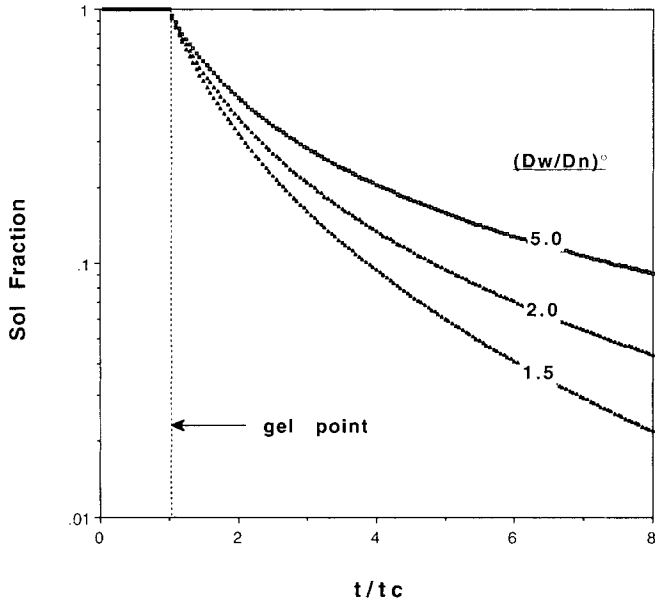

Figure 5. Effect of initial MWD on sol fraction for batch cross-linking.

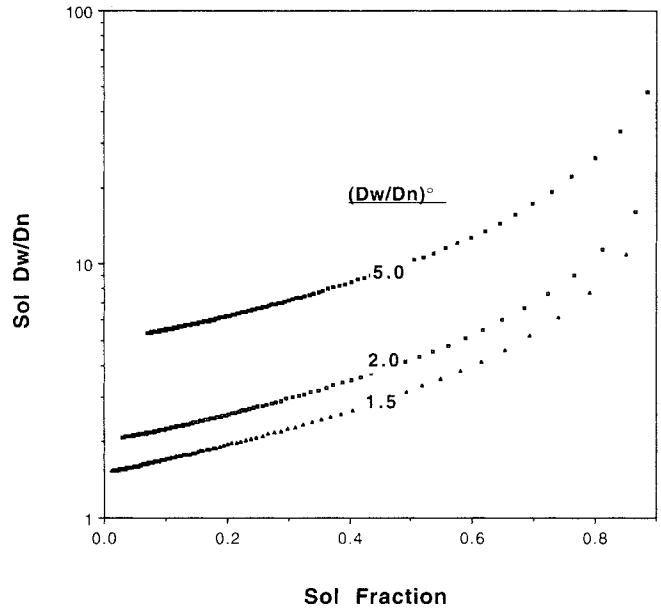

Figure 7. Effect of initial MWD on sol MWD.

first glance, it might appear to be a result of the closure method used in estimating the third moment of this generation. However, further investigation reveals that this result is truly independent of the closure method. An analytical proof is provided in the Appendix and confirms the validity of the closure method used.

We now turn our attention to chain coupling in CFST reactors, and first consider the dynamic reactor behavior during startups. In the earlier study (Cozewith et al., 1979), it was shown that in the pregel region, the time to reach steady state in D_w increased with θ_r (see Figure 8). For $\theta_r > 1$, the time from startup at which D_w became infinite was found to be given by

$$t_g/\theta = \left[\Pi - 2\tan^{-1}(\theta_r/2-1)/(\theta_r-1)^{1/2}\right]/(\theta_r-1)^{1/2} \quad (38)$$

where $\theta_r = \theta/\theta_c$.

However, it was not possible to calculate line out times in the post-gel region. Numerical fractionation model calculations of D_w and sol fraction for reactor startups with θ_r ranging from 1.12 to 20.0 are shown in Figures 9 and 10. The time to reach the gel point t_g/θ, as given by the time corresponding to the maximum in D_w (Figure 9), is in agreement with

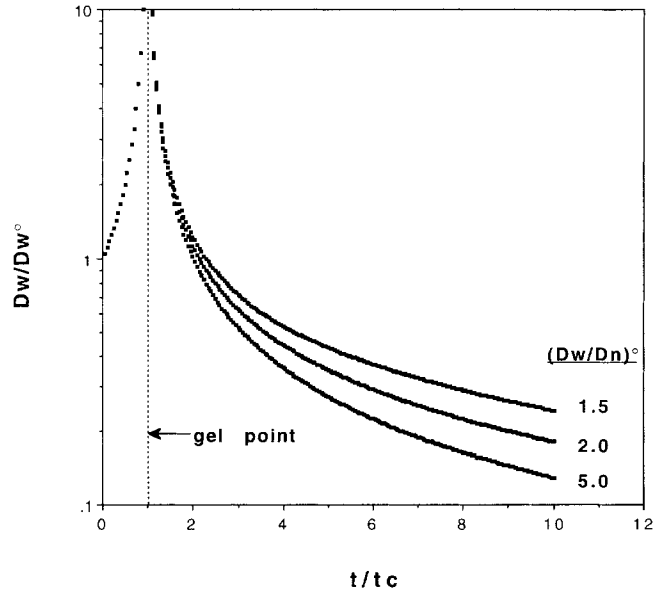

Figure 6. Effect of initial MWD on sol D_w for batch cross-linking.

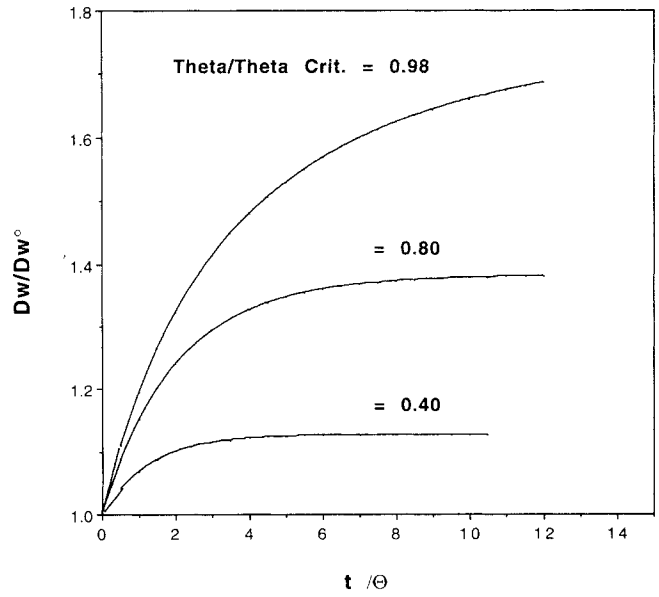

Figure 8. CFSTR startup in the pregel region.

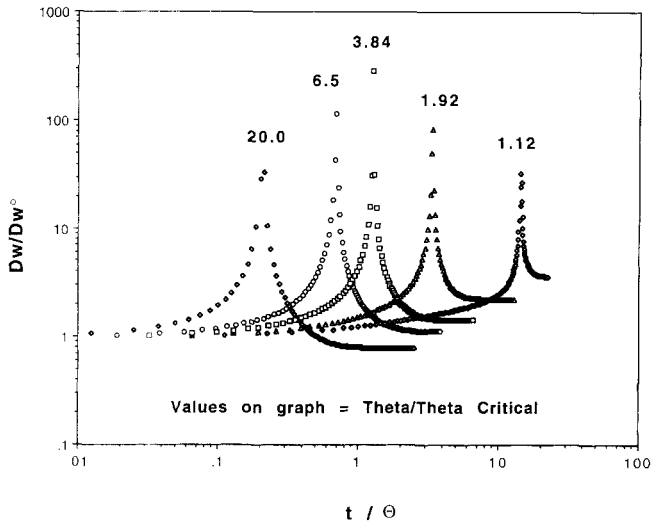

Figure 9. Sol D_w line out in a CFSTR.

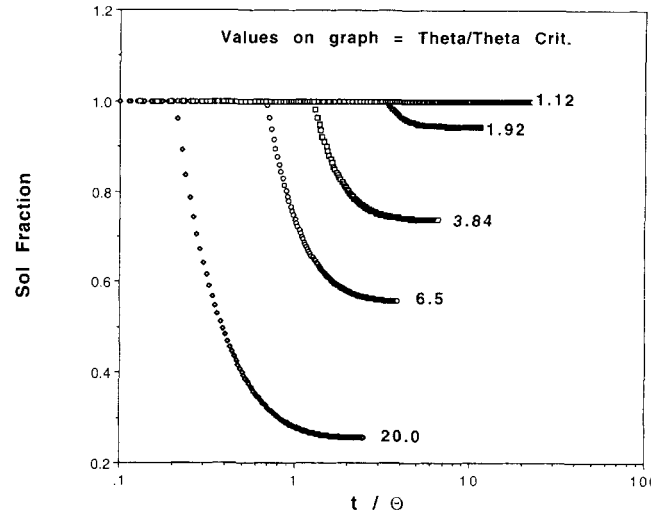

Figure 10. Sol fraction behavior for CFSTR startup.

values obtained from the exact solution (Eq. 38). The range of dynamic behavior illustrated in Figure 9 is quite remarkable. The time to line out D_w consists of the time to reach the gel point, t_g/θ plus the time for the sol to reach steady state following the gel point. This time is a function of θ_r, which is equal to $4k\theta Q_1^0 D_w^0$ and is indicative of the rate of the branching reaction. When θ_r is near 1, the rate is relatively low and it takes a long time for gel to form as can be seen from the t_g/θ value calculated from Eq. 38. Once gel does form, the sol D_w is lined out in an additional 3–4 reactor turnovers. At higher branching rates, and larger θ_r, the gel point is reached more rapidly, and line out time is reduced. For θ_r between 1 and 4, the time to steady state for a reactor startup is approximately equal to $(t_g/\theta + 3)$. Above θ_r equal to 4, line out times get shorter as θ_r increases. For example, when $\theta_r = 20$, only 1 turnover is needed past t_g/θ to reach steady state. This is a consequence of the very fast disappearance of the sol polymer by reaction which rapidly lowers the sol concentration in the reactor to the steady-state value.

The dynamic behavior of the sol fraction during reactor startup (see Figure 10) is similar to that of D_w. Once t/θ is greater than t_g/θ, the sol fraction decreases from 1.0 and reaches steady state in the same number of reactor turnovers as D_w.

Steady-state behavior for the CFST reactor was obtained by integrating the model ODEs out for a long enough time for the results to be time independent. Calculations were made for θ/θ_c between 1.12 and 100 with $(D_w/D_n)^0$ for the initial polymer ranging from 1.5 to 5.0. As shown in Figure 11, the steady-state sol fraction decreases very rapidly as θ/θ_c is increased to about 40, and then further increases in θ/θ_c have relatively little additional effect. D_w/D_w^0 in the CFST appears to be almost independent of the initial MWD. All of the calculated points in Figure 12 can be well correlated by a single curve. Thus, initial polymer MWD has a much greater influence on the course of the chain coupling reaction in a batch as compared to a CFST reactor. There is also a considerable difference in the behavior of D_w/D_n for the sol fraction. As the sol fraction concentration is reduced in the CFST, D_w/D_n passes through a minimum and then approaches an asymptotic value higher than $(D_w/D_n)^0$ (see Figure 13) rather than equal to $(D_w/D_n)^0$, as was the case for the batch reactor (Figure 7). For both reactor types, the sol fraction becomes dominated by branched first generation polymer at low sol levels. However, the residence time distribution in the CFST reactor is responsible for broadening the MWD, in comparison to the batch reactor.

The three product parameters that characterize the extent of cross-linking, D_w/D_w^0, D_w/D_n, and sol fraction, are all functions of only reaction time/initial reaction time (θ_r or t_r) once the initial polymer MWD is specified. Thus, D_w/D_w^0 and D_w/D_n for the sol have a unique relationship to the sol fraction as illustrated in Figure 14 for a polymer with $(D_w/D_n)^0$ equal to 2.0. The dependence of polymer properties on reduced reaction time allows determination of the branching

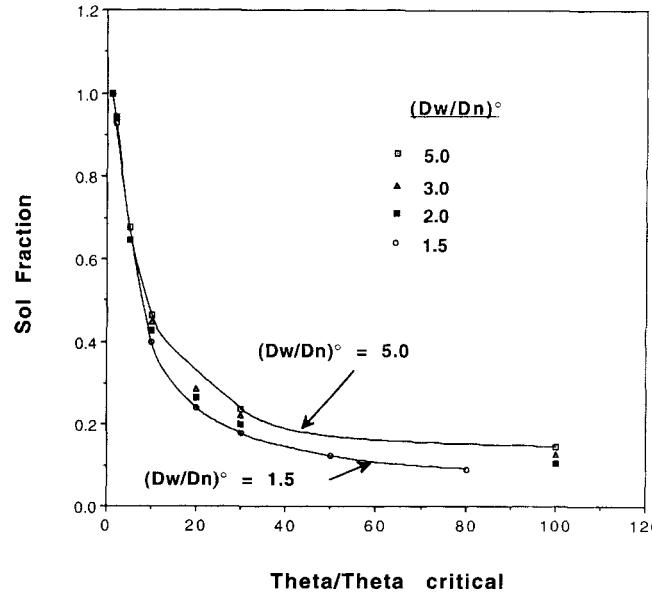

Figure 11. Effect of initial MWD on CFSTR sol fraction.

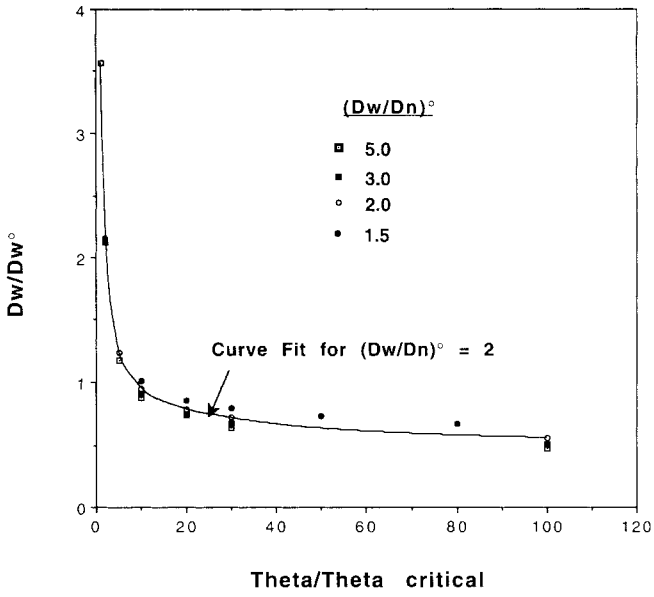

Figure 12. Effect of initial MWD on sol D_w in a CFSTR.

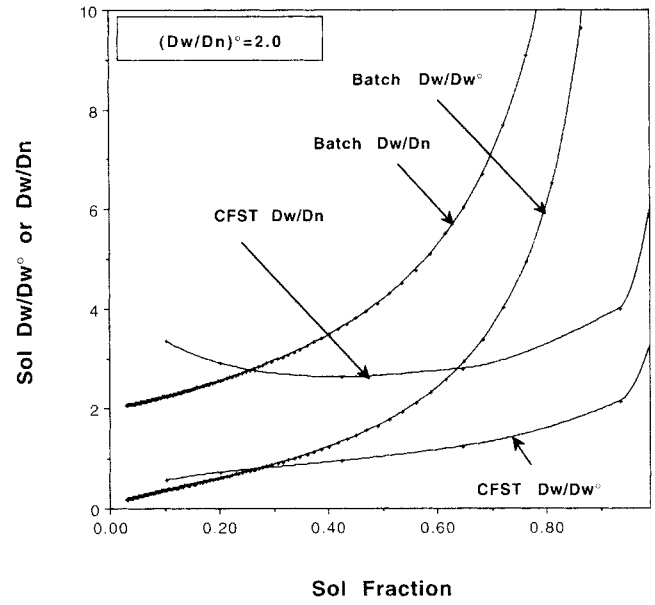

Figure 14. Comparison of sol fraction MW and MWD.

rate constant from a polymer analysis. For example, if a cross-linking reaction is carried out at known values of Q_1^0, θ or t, and D_w^0, extraction of the polymer to separate the gel and sol fractions followed by GPC measurement of the sol to obtain D_w/D_n and D_w should give results in agreement with Figure 14 when the branching kinetics are well represented by the assumed coupling mechanism. For branched chains, D_w measurement by GPC requires a detector that gives absolute D_w values, such as LALLS. θ_r or t_r can be obtained from either Figures 2 or 3 or Figures 11 or 12, depending on the reactor type. Once these parameters are determined, the branching rate constant k can readily be calculated.

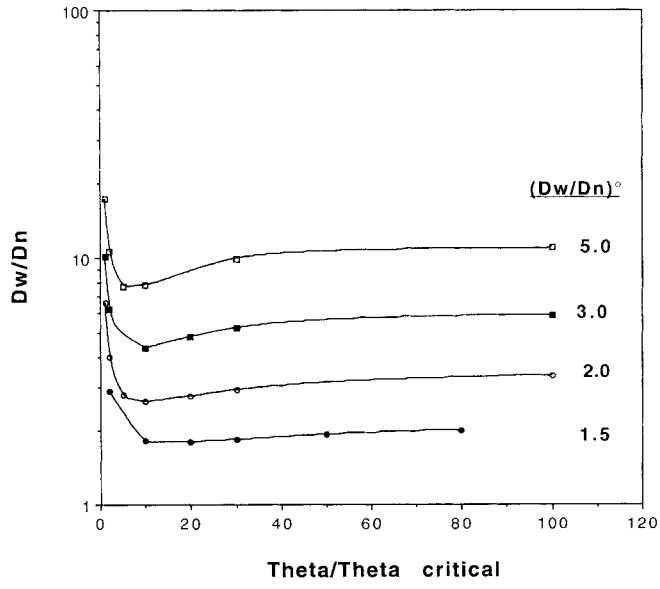

Figure 13. Effect of initial MWD on sol MWD in a CFSTR.

Conclusions

Describing reactor behavior for chain coupling reactions in the post gel region has been a challenging problem. The numerical fractionation technique, which is based on simple population balance concepts, seem well suited to modeling reactor performance and polymer properties. However, although the moment equations are readily derived, solution of the equations for the CFST reactor requires an ODE algorithm with a high degree of accuracy because of differences of many orders of magnitude in the values of terms appearing in the equation. For batch reactors, we have mapped the amount of sol fraction past the gel point, and the MW and MWD of the sol as a function of initial polymer D_w/D_n and reaction time t/t_c. D_w/D_n for the sol is at a maximum just past the gel point, and then drops rapidly as gelation proceeds, eventually returning to the initial value of D_w/D_n^0 as the sol fraction approaches zero. A comparison of the results to Flory's statistical derivation for random cross-linking showed good agreement between the predictions of both methods. This provides justification of the validity of the closure method used in numerical fractionation as it yields satisfactory predictions. Disagreement between the two methods is only significant in the vicinity of the gel point, where both are, by definition, in error.

Chain coupling in a CFST reactor results in a very diverse range of dynamic behavior. In the pre-gel region, reactor line out time lengthens as the residence time approaches the critical residence time, and in the vicinity of the critical residence time a large number of reactor turnovers are needed for the sol polymer molecular weight to reach steady state. In the post gel region, increases in residence time reduce the number of turnovers needed for reactor line out and for $\theta/\theta_c \geq 20$, steady state is attained in one turnover or less. We also show that batch and CFST reactors compared at equal reduced reaction times (θ/θ_c or t/t_c) give appreciably different characteristics in the post gel region. The coupling reaction proceeds faster in the batch reactor giving lower sol fractions

than the CFST reactor. On the other hand, at equal sol fraction, the sol fraction D_w is less in the CFST than the batch reactor, but D_w/D_n of the sol can be either higher or lower depending on the amount of sol.

Acknowledgment

We wish to thank the reviewers of this article for especially thorough and thoughtful reviews which resulted in a better article.

Notation

D_n = number average degree of polymerization
D_w = weight average degree of polymerization
p = parameter in the most probable distribution
$P_{y,i}$ = concentration of chains containing i mers, for generation y, mol/L
Q_n = nth moment of polymer MWD
$Q_{y,n}$ = nth moment of MWD for generation y
t_r = reduced reaction time
W_s = weight fraction of sol
Z_n = normalized moment, Q_n/Q_n^0
θ_r = normalized residence time, θ/θ_c

Literature Cited

Caracotsios, G. M., and W. E. Stewart, "Sensitivity Analysis of Initial Value Problems with Mixed ODE's and Algebraic Equations," *Comp. and Chem. Eng.*, **9**, 359 (1985).

Charlesby, A., "Gel Formation and Molecular Weight Distribution in Long Chain Polymers," *Proc. Roy. Soc. Ser. A*, **222**, 542 (1954).

Cozewith, C., W. W. Graessley, and G. Ver Strate, "Polymer Crosslinking in Continuous Flow Stirred Reactors," *Chem. Eng. Sci.*, **34**, 345 (1979).

Flory, P. J., "Molecular Size Distribution in Three Dimensional Polymers: V. Post-gelation Relationships," *J.A.C.S.*, **69**, 30 (1947).

Gossage, J. L., "Numerical Fractionation Modeling of Nonlinear Polymerization," PhD Thesis, Illinois Inst. of Technology, Chicago (1997).

Gossage, J. L., and F. Teymour, "Analysis of Radiation-Induced Polymer Crosslinking Using Numerical Fractionation," *Macromol.*, in press (1998).

Mikos, A. G., C. G. Takoudis, and N. A. Peppas, "Kinetic Modeling of Copolymerization/Cross-Linking Reactions," *Macromol.*, **19**, 2174 (1986).

Okay, O., "Kinetics of Gelation in Free Radical Crosslinking Copolymerization," *Polymer*, **35**, 2613 (1994).

Saidel, G. M., and S. Katz, "Dynamic Analysis of Branching in Radical Polymerization," *Poly. Sci., Poly. Phys. Ed.*, **6**, 1149 (1968).

Teymour, F., and J. D. Campbell, "Analysis of the Dynamics of Gelation in Polymerization Reactors Using the 'Numerical Fractionation' Technique," *Macromol.*, **27**, 2460 (1994).

Tobita, H., and A. E. Hamielec, "A Kinetic Model for Network Formation in Free Radical Polymerization," *Makromol. Chem. Macromol. Symp.*, **20/21**, 501 (1988).

Tobita, H., and A. E. Hamielec, "Modeling of Network Formation in Free Radical Polymerization," *Macromol.*, **22**, 3098 (1989).

Tobita, H., and A. E. Hamielec, "Control of Network Structure in Free-Radical Crosslinking Copolymerization," *Polymer*, **33**, 3647 (1992).

Tobita, H., Y. Yamamoto, and K. Ito, "Molecular Weight Distribution in Random Crosslinking of Polymers: Modality of the Molecular Weight Distribution," *Macromol. Theory Simul.*, **3**, 1033 (1994).

Xie, T., and A. E. Hamielec, "Modeling Free-Radical Copolymerization Kinetics: 3," *Makromol. Chem., Theory Simul.*, **2**, 777 (1993).

Zhu, S., and A. E. Hamielec, "Modeling of Free-Radical Polymerization with Cross-linking: Monoradical Assumption and Stationary-State Hypothesis," *Macromol.*, **26**, 3131 (1993).

Appendix

As discussed earlier in this article, the polydispersity of the *initial* linear polymer generation appears to be unaffected by the cross-linking reaction. This appendix will demonstrate that this phenomenon is not an artifact of the closure method employed in the equations and that it does hold for a wide class of distributions.

The population balance for the initial polymer generation is given by Eq. 9, which is rewritten here as

$$\frac{dP_{1,i}}{dt} = -kiP_{1,i}Q_1 \tag{A1}$$

If a scaled time τ equal to kQ_1t is introduced, this equation becomes

$$\frac{dP_{1,i}}{d\tau} = -iP_{1,i} \tag{A2}$$

which can be used to generate the moment equations for the initial polymer generation, as given by

$$\frac{dQ_{1,0}}{d\tau} = -Q_{1,1} \tag{A3}$$

$$\frac{dQ_{1,1}}{d\tau} = -Q_{1,2} \tag{A4}$$

$$\frac{dQ_{1,2}}{d\tau} = -Q_{1,3} \tag{A5}$$

The dynamic behavior of the polydispersity of this generation can thus be investigated either by solving the moment Eqs. A3–A5, or by directly solving the population balance Eq. A2. Both methods are illustrated here, starting with the former. First, the polydispersity of this generation is defined as

$$PD_1 = \frac{Q_{1,2}Q_{1,0}}{Q_{1,1}^2} \tag{A6}$$

which, after differentiation, yields

$$\frac{dPD_1}{d\tau} = \frac{Q_{1,0}}{Q_{1,1}^2}\left(\frac{dQ_{1,2}}{d\tau}\right) + \frac{Q_{1,2}}{Q_{1,1}^2}\left(\frac{dQ_{1,0}}{d\tau}\right) - 2\frac{Q_{1,2}Q_{1,0}}{Q_{1,1}^3}\left(\frac{dQ_{1,1}}{d\tau}\right) \tag{A7}$$

and after substitution using Eqs. A3–A5, becomes

$$\frac{dPD_1}{d\tau} = \frac{1}{Q_{1,1}^2}\left[-Q_{1,0}Q_{1,3} - Q_{1,2}Q_{1,1} + 2\frac{Q_{1,0}Q_{1,2}^2}{Q_{1,1}}\right] \tag{A8}$$

The righthand side of Eq. A8 obviously vanishes at all times as a direct result of the closure approximation (Eq. 25), and thus PD_1 remains invariant. It thus appears that the closure technique is forcing this behavior. However, it can be shown, by the direct solution of Eq. A2, that this behavior depends only on the shape of the initial distribution and that the validity of the closure technique is a result, not a cause, of this phenomenon.

Equation A2 can be directly integrated to yield

$$P_{1,i} = P_{1,i}(0)e^{-\tau i} \tag{A9}$$

which represents the chain length distribution of polymer in the linear generation as a function of scaled time τ and $P_{1,i}(0)$, the chain length distribution of the initial polymer. This can naturally be used to generate the distribution moments and hence calculate the polydispersity. If one invokes a continuous variable approximation, the moments can be expressed as integrals, and the following expression results for the polydispersity

$$PD_1 = \frac{\int_0^\infty P_{1,i}(0)e^{-\tau i}di \int_0^\infty i^2 P_{1,i}(0)e^{-\tau i}di}{\left(\int_0^\infty iP_{1,i}(0)e^{-\tau i}di\right)^2} \tag{A10}$$

To prove that this remains constant, one has to show that this expression is independent of τ. This is obviously not true for any arbitrary distribution $P_{1,i}(0)$, but can be shown to hold for specific distributions. For example, if the initial distribution can be fitted by a Schultz (Gamma) distribution, which is reasonable to expect under the assumption made in the text of a unimodal distribution for the initial polymer, then the desired result can be proven.

The Schultz weight fraction distribution (as in Teymour and Campbell, 1994) expresses the weight fraction of chains of length i as

$$W_i = \frac{y^{z+1}i^z e^{-yi}}{\Gamma(z+1)} \tag{A11}$$

where the parameters y and z are related to the polymer weight-average chain length $\bar{x}_w(0)$ and the polydispersity $PD_1(0)$, and are given by

$$z = \frac{1}{PD_1(0) - 1} \tag{A12}$$

$$y = \frac{z+1}{\bar{x}_w(0)} \tag{A13}$$

The molar concentration of chains of length i, $P_{1,i}(0)$ can thus be expressed as

$$P_{1,i}(0) = \frac{y^{z+1}i^{z-1}e^{-yi}}{\Gamma(z+1)}Q_1 \tag{A14}$$

and the zeroth-moment $Q_{1,0}$ of the linear generation can be expressed as

$$Q_{1,0} = \int_0^\infty \frac{y^{z+1}i^{z-1}e^{-yi}}{\Gamma(z+1)} Q_1 e^{-\tau i}di \tag{A15}$$

A simple variable transformation can be used to relate this moment to the initial zeroth-moment $Q_0(0)$, as given by

$$Q_{1,0} = \left(\frac{y}{y+\tau}\right)^z Q_0(0) \tag{A16}$$

Similarly, the first and second moments can be obtained

$$Q_{1,1} = z\frac{y^z}{(y+\tau)^{z+1}} Q_0(0) \tag{A17}$$

$$Q_{1,2} = z(z+1)\frac{y^z}{(y+\tau)^{z+2}} Q_0(0) \tag{A18}$$

Thus, the chain length averages of this generation can be shown to have the same dependence on τ as given by

$$\bar{x}_{n_1} = \frac{z}{y+\tau} \tag{A19}$$

and

$$\bar{x}_{w_1} = \frac{z+1}{y+\tau} \tag{A20}$$

Finally, the polydispersity can be calculated as

$$PD_1 = \frac{z+1}{z} = PD_1(0) \tag{A21}$$

which demonstrates that although the chain-length averages of the linear generation continuously decrease as a result of consumption by the cross-linking reaction, its polydispersity remains unaffected. Since this is shown to be independent of the closure method used, it also demonstrates the validity of this closure equation for this particular generation. Validation for other generations will be attempted elsewhere.

Manuscript received Apr. 9, 1997, and revision received Dec. 9, 1997.